Research Article | Vol. 13, No. 4 / 1 Apr 2022 / Biomedical Optics Express 2278
Biomedical Optics EXPRESS

Hybrid confocal Raman endomicroscopy for morpho-chemical tissue characterization

CONOR C. HORGAN,[1] MAGNUS JENSEN,[1] CIRO CHIAPPINI,[1,2] TOM VERCAUTEREN,[3] RICHARD COOK,[4] AND MADS S. BERGHOLT[1,*]

[1]Centre for Craniofacial and Regenerative Biology, King's College London, London SE1 9RT, UK
[2]London Centre for Nanotechnology, King's College London, London WC2R 2LS, UK
[3]School of Biomedical Engineering and Imaging Sciences, King's College London, London WC2R 2LS, UK
[4]Centre for Oral, Clinical and Translational Sciences, King's College London, London SE1 9RT, UK
*mads.bergholt@kcl.ac.uk

Abstract: Confocal laser endomicroscopy (CLE) offers imaging of tissue microarchitecture and has emerged as a promising tool for *in vivo* clinical diagnosis of cancer across many organs. CLE, however, can show high inter-observer dependency and does not provide information about tissue molecular composition. In contrast, Raman spectroscopy is a label-free optical technique that provides detailed biomolecular compositional information but offers limited or no morphological information. Here we present a novel hybrid fiber-optic confocal Raman endomicroscopy system for morpho-chemical tissue imaging and analysis. The developed confocal endomicroscopy system is based on a novel detection scheme for rejecting Raman silica fiber interference permitting simultaneous CLE imaging and Raman spectral acquisition of tissues through a coherent fiber bundle. We show that this technique enables real-time microscopic visualization of tissue architecture as well as simultaneous pointwise label-free biomolecular characterization and fingerprinting of tissue paving the way for multimodal diagnostics at endoscopy.

1. Introduction

Confocal laser endomicroscopy (CLE) has emerged as a powerful clinical tool for the *in vivo* assessment of tissue microarchitecture during clinical examinations [1]. In CLE, a confocal fluorescence image is generated using a fluorescent contrast agent that is relayed through a coherent fiber bundle with a miniature microscope objective at the distal tip, enabling video-rate imaging of tissue morphology on micron scales through endoscopes. CLE has been applied to a variety of tissues *in vivo* for clinical and diagnostic applications of cancer including in the esophagus, stomach, and colon [2–4]. While confocal endomicroscopy is very promising and enables incredibly detailed visualization of cell/tissue architecture and morphology *in vivo*, CLE images do not provide biomolecular tissue information and their interpretation can be highly subjective [5,6]. Diseases such as cancers are fundamentally associated with changes in molecular composition (e.g., increased DNA content and overexpression of certain proteins) and CLE is not able to capture this important information.

Raman spectroscopy is a vibrational analytical technique based on the premise of inelastic light scattering. The Raman spectrum of tissue provides detailed insights into the biomolecular composition such as proteins, lipids, and DNA [7]. For this reason, it can serve as an optical biopsy and is currently under clinical validation for the detection and diagnosis of diseased or cancerous tissues across multiple clinical endoscopic applications [8–10]. However, while Raman endoscopy provides a wealth of biomolecular information, the weak Raman scattering signal does not enable real-time imaging and hence no visual structural data can be obtained [11]. This is because acquisition times are on the order of seconds or sub seconds per spectrum. Raster scanning tissues *in vivo* in clinical settings is not a feasible approach, and while Raman imaging through fibers has been demonstrated, this approach remains unsuitable for clinical endoscopic

#449110 https://doi.org/10.1364/BOE.449110
Journal © 2022 Received 1 Dec 2021; revised 6 Feb 2022; accepted 9 Feb 2022; published 21 Mar 2022

Biomedical Optics EXPRESS

application [12]. As such, Raman spectroscopy is currently limited to pointwise spectra acquired from the tissue.

Given the limitations of both CLE and Raman endoscopy, there is an unmet need to develop multimodal strategies that offers more comprehensive characterization of tissues at both the morphological and biomolecular level. Multimodal imaging is being increasingly accepted as an important development in medicine, and indeed Raman spectroscopy has previously been combined with widefield/fluorescence imaging and optical coherence tomography towards improved diagnostic imaging [11,13,14]. The combination of CLE and Raman spectroscopy could enable clinicians to simultaneously obtain highly complementary morphological structure and biochemical tissue information at the microscopic level. However, there are several technical difficulties that must be resolved for the development of such a multimodal technique: 1) Endomicroscopy utilizes coherent fiber bundles and has no dedicated excitation fibers or distal optical filters. 2) Coupling a Raman excitation laser into fiber bundles generates a strong silica background signal that overwhelms tissue Raman signals. 3) Conventional Raman endoscopic probes require dedicated long-pass and band-filters at the distal tip of the fiber probes. 4) Fluorescent agents used for CLE (e.g., fluorescein) could interfere with the Raman spectral range.

Here, we develop a novel approach to overcome these difficulties without significantly compromising Raman signal or CLE imaging quality. We construct a multimodal hybrid confocal Raman and CLE system that allows us to overcome the key challenges and simultaneously acquire video-rate CLE and pointwise Raman spectra of tissues.

2. Methods

2.1. Hybrid confocal Raman endomicroscopy instrumentation

The developed prototype hybrid confocal Raman endomicroscopic imaging system (Fig. 1) consists of a custom-built confocal scanning platform integrated with a 785 nm excitation Raman module. The insert (Fig. 1) shows the spectral ranges that we employ: the contrast agent emitting fluorescence is excited at 488 nm and emits above 500 nm while the Raman signal is excited in the near-infrared (NIR) region at 785 nm and detected >1000 nm (high wavenumber Raman spectroscopy) to prevent the tissue and silica Raman/fluorescence spectral tail interfering with the Raman signal. The confocal scanning platform uses a 488 nm Sapphire laser (Toptica iBeam Smart 488) for confocal fluorescence imaging and a frequency-stabilized 785 nm diode laser for Raman spectroscopy (B&W Tek BRM-785-0.55-100-0.22-FC, 600 mW). Confocal fluorescence images are generated through an 8 kHz galvo-resonant scanner (Thorlabs LSK-GR08), controlled using a data acquisition system (National Instruments PXIe-1073 and NI-5732). Detection of confocal scanned signal is achieved by filtering the fluorescence light using a 495 nm dichroic mirror (Semrock FF495-DiO2) and focusing it onto a 100 μm fiber (Thorlabs), acting as a pinhole. The same fiber was coupled to a PMT (PMTTS, Thorlabs) and a current-to-voltage converter (PMTTS, Thorlabs) for signal detection. A dichroic mirror (Semrock Di02-R785) reflecting wavelengths above 785 nm is used to separate the Raman scattered light from Rayleigh scattering, while another dichroic mirror reflects wavelengths below 750 nm (Semrock FF750-SDi02) and is used to couple the Raman laser excitation and collection into the confocal optical axis.

Using a novel detection scheme, we reduce the silica Raman interference signal originating from the coherent fiber bundle. Our detection scheme consists of a custom (circular to linear) fiber bundle. The 785 nm laser light is focused into a small spot on the central part of the coherent fiber bundle (Fig. 1). The directly backscattered Raman/fluorescence light from the silica fiber is collected by the same objective, transmitted and focused onto the central part of the circle using the second objective and is therefore not coupled into the spectrometer. This ring configuration effectively discards Raman/fluorescence fiber light originating from the focused 785 nm laser on the central area of the coherent fiber bundle. The 785 nm laser light is in this way able to be coupled into and propagate through the coherent fiber bundle to the distal miniature

Biomedical Optics EXPRESS

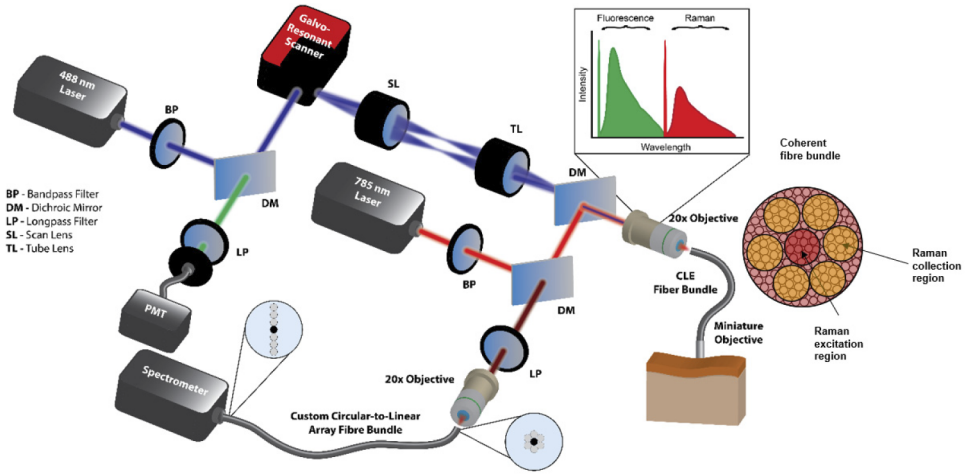

Fig. 1. Schematic of the hybrid confocal Raman endomicroscopic system. The system comprises an integrated 488 nm confocal microscope for morphological imaging and a NIR Raman module for molecular characterization. Using a custom circular to linear fiber bundle with a deactivated central fiber for spectrometer coupling we reduce the directly scattered silica Raman signal originating from the central part of the coherent fiber bundle.

microscope. Detection of the Raman signal while rejecting the fiber bundle background signal is performed by focusing the scattered light onto the custom fiber bundle (Thorlabs). The fiber bundle comprises a linear array of 6×100 µm fibers matched to the input slit of a fiber-coupled scientific grade spectrograph (Ocean Optics QEPro) equipped with gold coated reflective mirror, a thermo electric-cooled NIR-optimized charge-coupled device (CCD) chip with a dynamic range of 200,000 photon counts (Hamamatsu). All CLE images reported in the work is acquired using a commercial coherent fiber bundle with a distal miniature microscope objective (Mauna Kea Technologies).

2.2. *Software for real-time video-rate CLE imaging and pointwise Raman measurements*

We have developed a comprehensive extension of the publicly available ScanImage (Vidrio) software for the synchronization of scanning and detection functions for CLE imaging in the Matlab scripting environment (Mathworks). The Vidrio software supports the National Instruments PXIe-1073 and NI-5732 boards used for synchronization between the galvo-resonant scanner and PMT. Raman spectral acquisition is also being performed through the Matlab software using the Omni-driver interface (Ocean Insight) for direct imaging and correlation between CLE images and Raman spectra. The acquisition software enables standard Raman spectral analysis in real-time including data preprocessing such as silica fiber background subtraction, baseline subtraction (Whittaker, lambda = 100000), Savitzky-Golay filtering (1 order, window = 5 px) and normalization to the integrated area.

3. Results

3.1. *Simultaneous CLE and pointwise Raman spectroscopy of tissues*

We first tested the developed system (Fig. 2(a)-(b)) on white optical tissue paper that is known to emit autofluorescence under 488 nm excitation (incident laser power = 0.2 mW). Video-rate CLE autofluorescence imaging of unlabeled tissue paper enabled real-time visualization of the microscopic tissue fibers showing that the system is capable of confocal imaging (Fig. 2(c)).

Biomedical Optics EXPRESS

To demonstrate the capability of our hybrid confocal Raman endomicroscopic system for simultaneous morphological and biomolecular tissue analysis, we applied our system to the skin and tissue of a healthy human volunteer. Informed consent was obtained by the subject (Ethics number 11/LO/0354). We performed simultaneous video-rate CLE imaging (30 frames/s, incident laser power = 0.2 mW)) and pointwise 785 nm Raman spectral measurements (integration time = 2 s, incident laser power = 24 mW) (Fig. 2(d)). CLE autofluorescence imaging of unlabeled skin tissues displayed limited details as expected due to lack of contrast agent. Despite the limited CLE contrast of unstained tissues, Raman spectra acquired during real-time CLE imaging (integration time = 2 s) from the center of the CLE field of view demonstrated signal in the high wavenumber region and enabled easy discrimination of skin and nail tissues (Fig. 2(d)). For instance, intense Raman peaks were identified at 2870 cm^{-1} (CH_2 stretching of lipids), 2930 cm^{-1} (CH_3 stretching of proteins), and 2970 cm^{-1} (CH_2 stretching). These peaks are well known to be present in tissue and have been reported in numerous studies and correlate with the major biological constituents of tissues including proteins and lipids. Importantly these protein and lipid related peaks in the high wavenumber have previously shown to be highly predictive of cancerous tissues across multiple organs [15,16]. Hence the hybrid confocal Raman endomicroscopy platform providing multiple sources of information has great potential to provide complementary diagnostic information.

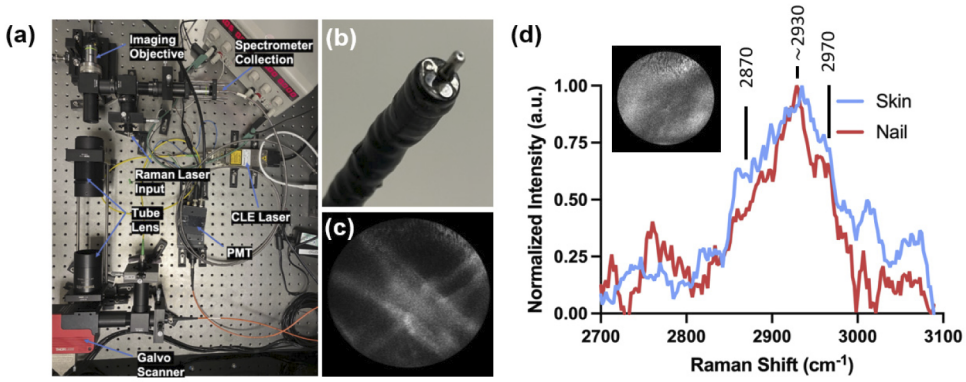

Fig. 2. (a) Optical setup of the hybrid Raman CLE system (b) The coherent fiber bundle compatible with endoscopes. (c) Confocal endomicroscopy imaging of optical lens tissue showing the individual fibers (d) High wavenumber Raman spectra of human skin and nail tissue of acquired through the CLE coherent fiber bundle during CLE imaging. Also shown is CLE autofluorescence image of unstained human skin tissue.

3.2. Evaluating the impact of fluorescein contrast agent on tissue Raman spectra

Intravenous fluorescein injection is often used as contrast agent for CLE imaging in patients. We next investigated whether topically applied fluorescein, used to achieve CLE imaging contrast, impacted the observed Raman signal. We topically applied fluorescein across different regions of porcine tissue and performed simultaneous CLE imaging and Raman spectral measurements (Fig. 3, Visualization 1). Topical application of fluorescein enabled the acquisition of higher quality confocal tissue images, highlighting the microscopic architecture of the porcine tissue (Fig. 3(a)). Raman spectra (integration time = 2 s) could be acquired during real-time CLE imaging and demonstrated strong signal in the high wavenumber region enabling discrimination of muscle and fat tissues (Fig. 3(b)). It is well known that muscle tissue shows weak signals while lipid rich tissue gives strong Raman signals due to the large scattering cross section of lipids. We also depict the raw Raman signals of muscle and fat tissue as well as the background

Biomedical Optics EXPRESS

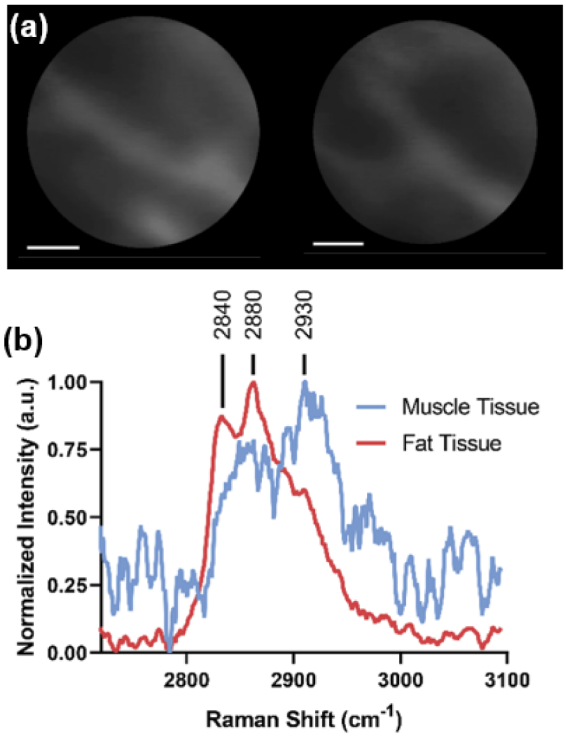

Fig. 3. (a) CLE images of fluorescein-labeled porcine tissue. (b) Normalized high wavenumber Raman spectra of fluorescein-labeled porcine muscle and fat tissues acquired through the coherent fiber bundle during CLE imaging. Scale bars = 50 µm.

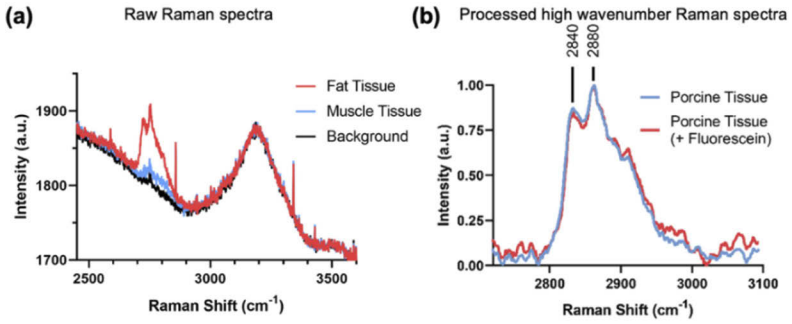

Fig. 4. (a) Raw Raman spectra of porcine fat/muscle tissue acquired through the coherent fiber bundle during CLE imaging. These have no background subtraction or smoothing. Also shown is the background signal of the system (b) Processed (baseline subtracted and normalized) high wavenumber Raman spectra of porcine tissue with and without fluorescein labeling acquired through the coherent fiber bundle during CLE imaging.

signal of the fiber (Fig. 4(a)). These results show that the background signal of the system gives rise to a large band near 3200 cm^{-1}. The origin of this band is not clear but importantly it does not interfere with the much more important bands of proteins, lipids and DNA near 2700-3000 cm^{-1}. Finally, we investigated whether the Raman spectral signal of tissue was affected by the presence of topically applied fluorescein. We found that fluorescein gives rise to a minor and almost negligible background increase (Fig. 4(b)). This is largely due to the separation of the

Biomedical Optics EXPRESS

Raman scattering signal in the NIR region from the fluorescence signal in the visible region (Fig. 1). While this might be more pronounced for muscle tissue due to relative weaker signal compared to fat, we think this represents a minor confounding factor similar in magnitude to e.g., peristaltic motion or tissue autofluorescence associated with *in vivo* applications [8]. Importantly, we observed minimal to no loss in Raman spectral signal strength or CLE imaging quality due to the simultaneous operation of both Raman spectral acquisition and CLE imaging.

4. Discussion

Multimodal diagnostics is becoming increasingly important in healthcare. The main aim of this work was to develop a new approach to perform multimodal morphological and biochemical imaging at endoscopy. The diagnostic capability of CLE and Raman endoscopy has already been extensively explored in the literature *ex vivo* and *in vivo*. Our hybrid confocal Raman endomicroscopy system combines two complementary techniques for simultaneous morphological tissue assessment and biochemical characterization. This system represents, to the best of our knowledge, the first demonstration of Raman spectral acquisition through a coherent fiber bundle with a miniature microscope at the tip without the use of optical filters, minimizing potential manufacturing complexity. We achieve this by combining a novel, custom-built circular to linear fiber bundle with high wavenumber Raman spectroscopy to reduce background fiber signal and minimize silica spectral overlap with tissue information. Differences in the wavelengths used for Raman spectroscopy (>1000 nm) and CLE imaging (>500 nm) can induce chromatic aberrations, and together with the absorption/scattering profile of biological tissues this will likely result in slightly different penetration depths for the two modalities (CLE penetration depth: <100 µm [17], Raman penetration depth: ~>100 µm [18] depending on the specific CLE probe). It is very difficult to estimate this precisely for tissue and this requires extensive Monte Carlo simulations considering the proprietary miniature microscope design. While CLE imaging enables visualization of surface lesions or the basement membrane of tissues, Raman spectroscopy enables simultaneous biochemical characterization of the tissue. Importantly, by avoiding the use of distal optical filters, our approach enables seamless incorporation of Raman spectroscopy into existing clinically approved CLE probes. Indeed, here we demonstrated the performance of our hybrid system using a commercial CLE fiber bundle (Mauna Kea Technologies). Incorporating Raman spectroscopy in this modular manner into systems with existing clinical approvals is likely to significantly simplify the process of clinical translation of a combined Raman-CLE endoscopic system.

Here, we also validated the impact of fluorescein using topical application on tissue. This does not represent a fully realistically scenario as often fluorescein is applied intravenously in the clinic. However, the concentrations used here approximate well or exceed the distribution found in tissue. We have previously observed in *in vivo* clinical trials [8] that intravenous injection of fluorescein has little or no effect on Raman spectra acquired in the high wavenumber NIR spectral range.

While our proposed hybrid system offers numerous advantages, it does face several limitations. Firstly, we need to further optimize the throughput of the system. Based on our experience, clinical Raman endoscopy acquisitions should be performed in less than a second to avoid motion artefacts and provide rapid diagnostic feedback for clinicians. This would certainly be achievable using a higher end spectrometer with lower F-number and more sensitive CCD as previously employed for Raman endoscopy [8]. Secondly, our CLE imaging clearly shows tissue structure in real-time, although with limited tissue details. However, state-of-the art CLE combined with suitable image processing techniques could improve this significantly. The main aim of this work was to develop a multimodal technique and show this can be applied to tissue for the first time. Thirdly, to reduce the background fiber bundle signal, Raman spectroscopy here is limited to the high wavenumber range. Though this reduces the extent of spectral information available, several

Biomedical Optics EXPRESS

studies have demonstrated the capacity of high wavenumber Raman spectroscopy for *in vivo* cancer diagnostics [9,15,19]. An increased DNA and upregulated protein to lipid ratio has often been associated with cancers. Finally, it is important to note that CLE generates images with a small FOV and Raman spectral acquisitions are obtained from the center of this FOV. Similarly, while CLE can achieve video rate imaging of this FOV, Raman spectroscopy necessitates longer spectral acquisitions. As such, *in vivo* application of our hybrid confocal Raman endomicroscopy system would likely need to rely on a snapshot imaging approach for diagnostic purposes. Importantly, the development of data fusion algorithm for extracting complementary CLE imaging information and combining it with molecular information represents an important future development towards applications in humans *in vivo*. The validation of this hybrid technique for improving the diagnosis of cancer compared to CLE and Raman endoscopy respectively requires a comprehensive study with possible hundreds of patients.

5. Conclusions

In summary, we have developed a hybrid confocal Raman endomicroscopy system for morpho-chemical tissue analysis. We have demonstrated that complementary real-time CLE imaging and pointwise Raman spectra can simultaneously be acquired with a view towards future *in vivo* clinical diagnostic applications. Importantly, our novel detection scheme enables easy integration with existing CLE probes, likely to streamline clinical translation processes. The development of multimodal approaches for diagnostics represents an important step to take advantage of the complementarity of the wealth of different techniques in biophotonics.

Funding. European Research Council under the European Union's Horizon 2020 research and innovation programme (grant agreement No.802778).

Disclosures. TV is founding director and shareholder of Hypervision Surgical Ltd and holds shares from Mauna Kea Technologies.

Data availability. Data underlying the results presented in this paper are not publicly available at this time but may be obtained from the authors upon reasonable request.

References

1. M. B. Wallace and P. Fockens, "Probe-based confocal laser endomicroscopy," Gastroenterology **136**(5), 1509–1513 (2009).
2. P. Sharma, A. R. Meining, E. Coron, C. J. Lightdale, H. C. Wolfsen, A. Bansal, M. Bajbouj, J. P. Galmiche, J. A. Abrams, A. Rastogi, N. Gupta, J. E. Michalek, G. Y. Lauwers, and M. B. Wallace, "Real-time increased detection of neoplastic tissue in Barrett's esophagus with probe-based confocal laser endomicroscopy: Final results of an international multicenter, prospective, randomized, controlled trial," Gastrointest. Endosc. **74**(3), 465–472 (2011).
3. W. B. Li, X. L. Zuo, C. Q. Li, F. Zuo, X. M. Gu, T. Yu, C. L. Chu, T. G. Zhang, and Y. Q. Li, "Diagnostic value of confocal laser endomicroscopy for gastric superficial cancerous lesions," Gut **60**(3), 299–306 (2011).
4. A. M. Buchner, M. W. Shahid, M. G. Heckman, M. Krishna, M. Ghabril, M. Hasan, J. E. Crook, V. Gomez, M. Raimondo, T. Woodward, H. C. Wolfsen, and M. B. Wallace, "Comparison of probe-based confocal laser endomicroscopy with virtual chromoendoscopy for classification of colon polyps," Gastroenterology **138**(3), 834–842 (2010).
5. M. B. Sturm and T. D. Wang, "Emerging optical methods for surveillance of Barrett's oesophagus," Gut **64**(11), 1816–1823 (2015).
6. T. C. Chang, J. J. Liu, S. T. Hsiao, Y. Pan, K. E. Mach, J. T. Leppert, J. K. McKenney, R. V. Rouse, and J. C. Liao, "Interobserver agreement of confocal laser endomicroscopy for bladder cancer," J. Endourol. **27**(5), 598–603 (2013).
7. C. Krafft, M. Schmitt, I. W. Schie, D. Cialla-May, C. Matthäus, T. Bocklitz, and J. Popp, "Label-free molecular imaging of biological cells and tissues by linear and nonlinear Raman spectroscopic approaches," Angew. Chemie - Int. Ed. **56**(16), 4392–4430 (2017).
8. M. S. Bergholt, W. Zheng, K. Y. Ho, M. Teh, K. G. Yeoh, J. Bok, Y. So, A. Shabbir, and Z. Huang, "Fiberoptic confocal Raman spectroscopy for real-time in vivo diagnosis of dysplasia in Barrett's Esophagus," Gastroenterology **146**(1), 27–32 (2014).
9. M. A. Short, W. Wang, I. T. Tai, and H. Zeng, "Development and in vivo testing of a high frequency endoscopic Raman spectroscopy system for potential applications in the detection of early colonic neoplasia," J. Biophotonics **9**(1-2), 44–48 (2016).

Biomedical Optics EXPRESS

10. I. J. Pence, D. B. Beaulieu, S. N. Horst, X. Bi, A. J. Herline, D. A. Schwartz, and A. Mahadevan-Jansen, "Clinical characterization of in vivo inflammatory bowel disease with Raman spectroscopy," Biomed. Opt. Express **8**(2), 524 (2017).
11. C. Horgan, M. S. Bergholt, M. Z. Thin, A. Nagelkerke, R. Kennedy, T. L. Kalber, D. J. Stuckey, and M. M. Stevens, "Image-guided Raman spectroscopy probe-tracking for tumor margin delineation," J. Biomed. Opt. **26**(03), 036002 (2021).
12. I. Gusachenko, M. Chen, and K. Dholakia, "Raman imaging through a single multimode fibre," Opt. Express **25**(12), 13782 (2017).
13. M. Chen, J. Mas, L. H. Forbes, M. R. Andrews, and K. Dholakia, "Depth-resolved multimodal imaging: Wavelength modulated spatially offset Raman spectroscopy with optical coherence tomography," J. Biophotonics **11**(1), e201700129 (2018).
14. C. A. Patil, N. Bosschaart, M. D. Keller, T. G. Van Leeuwen, and A. Mahadevan-jansen, "Combined Raman spectroscopy and optical coherence tomography device for tissue characterization," Opt. Lett. **33**(10), 1135–1137 (2008).
15. M. S. Bergholt, K. Lin, J. Wang, W. Zheng, H. Xu, Q. Huang, J. lin Ren, K. Y. Ho, M. Teh, S. Srivastava, B. Wong, K. G. Yeoh, and Z. Huang, "Simultaneous fingerprint and high-wavenumber fiber-optic Raman spectroscopy enhances real-time in vivo diagnosis of adenomatous polyps during colonoscopy," J. Biophotonics **9**(4), 333–342 (2016).
16. Z. Movasaghi, S. Rehman, and I. U. Rehman, "Raman spectroscopy of biological tissues," Appl. Spectrosc. Rev. **42**(5), 493–541 (2007).
17. G. D. De Palma, "Confocal laser endomicroscopy in the "in vivo" histological diagnosis of the gastrointestinal tract," World J. Gastroenterol. **15**(46), 5770–5775 (2009).
18. P. Matousek and N. Stone, "Emerging concepts in deep Raman spectroscopy of biological tissue," Analyst **134**(6), 1058–1066 (2009).
19. E. M. Barroso, R. W. H. Smits, T. C. B. Schut, I. Ten Hove, J. A. Hardillo, E. B. Wolvius, R. J. B. De Jong, S. Koljenović, and G. J. Puppels, "Discrimination between oral cancer and healthy tissue based on water content determined by Raman spectroscopy," Anal. Chem. **87**(4), 2419–2426 (2015).